Effective control of photoluminescence from ZnO nanowires by a-SiN_x:H decoration

Rui Huang,[1,2] Shuigang Xu,[1] Xiang Wang,[2] Wenhao Guo,[1] Chao Song,[2] Jie Song,[2] Kin Ming Ho,[1] Shengwang Du,[1] and Ning Wang[1,*]

[1]*Department of Physics and the William Mong Institute of Nano Science and Technology, Hong Kong University of Science and Technology, Clear Water Bay, Kowloon, Hong Kong, China*

[2]*Department of Physics and Electronic Engineering, Hanshan Normal University, Chaozho, 521041, China*

**Corresponding author: phwang@ust.hk*

Received October 17, 2011; revised November 11, 2011; accepted November 11, 2011; posted November 23, 2011 (Doc. ID 156667); published January 12, 2012

The a-SiN_x:H with a large bandgap of 3.8 eV was utilized to decorate ZnO nanowires. The UV emission from the a-SiN_x:H-decorated ZnO nanowires are greatly enhanced compared with the undecorated ZnO nanowire. The deep-level defect emission has been completely suppressed even though the sample was annealed at temperatures up to 400 °C. The incorporation of H and N is suggested to passivate the defect states at the nanowire surface and thus result in the flat-band effect near ZnO surface as well as reduction of the nonradiative recombination probability.

OCIS Codes: 160.2540, 160.4760, 220.4241, 250.5230.

Nanowires have attracted great interest over the past decade because of their unique physical properties and great potential as building blocks for next-generation nanoelectronic devices. Among the reported quasi-one-dimensional (1D) nanostructures, ZnO is thought to be one of the most promising candidates for LEDs because of its wide direct bandgap as well as large exciton binding energy [1–3]. The preparation and optical properties of ZnO 1D nanostructures have already been described in many reports [1–5]. The room-temperature photoluminescence of ZnO typically consists of UV emission from free exciton recombination and a broad visible emission associated with intrinsic or extrinsic defects [6]. It is evident that the presence of defects would significantly deteriorate the UV emission efficiency of the ZnO devices. On the other hand, the strong surface effect due to the high surface-to-volume ratio also enhances the surface recombination losses. As a result, the unpassivated surface states serve as nonradiative recombination centers and thus lower the luminescence efficiency of devices. Therefore, controlling defect states and completely eliminating the defect-related emission become the key issues for improving the UV emission efficiency. Up to now, suppression of the defect emission and enhancement of the UV emission has been realized by various methods, including plasma treatment and formation of core-shell structures with wide bandgap materials or polymers [7–13]. However, in most cases, the defect emission still cannot be totally eliminated [7–10], and more seriously, it would be recovered at the annealing temperatures above 400 °C, especially for those treated by plasma [12].

In this Letter, we report on the enhancement of PL properties and thermal stability of ZnO-core/a-SiN_x:H-shell nanowires. The mechanism for the improvement of ZnO nanowire PL characteristics is discussed and attributed to the surface modification by a-SiN_x:H where H and N atoms play important roles.

The preparation of ZnO-core/a-SiN_x:H shell nanowires consists of two steps. First, ZnO nanowires were prepared by the chemical vapor transport method on a silicon substrate as reported elsewhere [14–16]. Then, the ZnO nanowires were directly coated with a-SiN_x:H by using the plasma-enhanced chemical vapor deposition technique with a high frequency (40.68 MHz). The a-SiN_x:H layer was prepared from silane diluted with ammonia and hydrogen at a low temperature of 250 °C. The flow rate of SiH_4, NH_3, and H_2 was 5, 25 and 30 sccm, respectively. According to the transmission spectrum and Tauc equation [17], the optical band gap of a-SiN_x:H is estimated to be 3.8 eV. The structure of the nanowires was characterized by a Philips XL30 scanning electron microscope (SEM), Raith e_LiNE nanoengineering workstation, and a JEOL high-resolution transmission electron microscope (HRTEM, 2010F). PL measurement was conducted by near-field scanning optical microscope (Nanonics Cryoview2000) equipped with a 1.5 mW He–Cd laser ($\lambda = 325$ nm) at room temperature. A Fourier transform IR (FTIR) spectroscope was used to record bonding configurations of a-SiN_x:H.

Figure 1(a) shows a SEM image of ZnO-core/SiN_x:H-shell nanowires, which displays that ZnO nanowires have uniform a-SiN_x:H covers. The fact that no a-SiN_x:H was packed in the interspaces of the nanowires indicates that a-SiN_x:H is preferentially grown on the surface of ZnO nanowires. The low-magnification TEM images of the ZnO-core/a-SiN_x:H-shell nanowire shown in Fig. 1(b) further reveals that a well-aligned a-SiN_x:H shell layer was coated on the ZnO-core nanowire. The local HRTEM in Fig. 1(c) manifests the microstructure of the boundary between the core and the shell. It is clear that the a-SiN_x:H shell with a thickness of 6 nm is of an amorphous structure, while the core is ZnO wurtzite structure with a lattice plane spacing of 0.52 nm as marked in Fig. 1, which corresponds to the (0001)-plane, indicating the growth direction is along the *C* axis.

Figure 2 shows the PL spectra obtained from the as-synthesized ZnO nanowires with and without a-SiN_x:H decoration, respectively. For the as-grown ZnO nanowires, one can see that the PL spectrum contains two typical emission peaks, the sharp UV emission near 380 nm and the broad green emission centered at 530 nm. Compared to the as-grown ZnO nanowire, the PL spectra taken from the ZnO-core/a-SiN_x:H-shell nanowires show very different features. First, the total

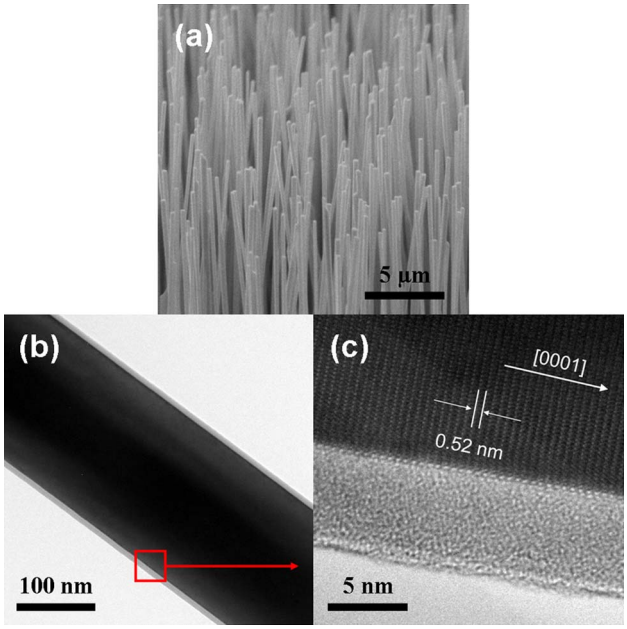

Fig. 1. (Color online) (a) SEM, (b) TEM, (c) HRTEM image of ZnO-core/a-SiN_x:H-shell nanowires.

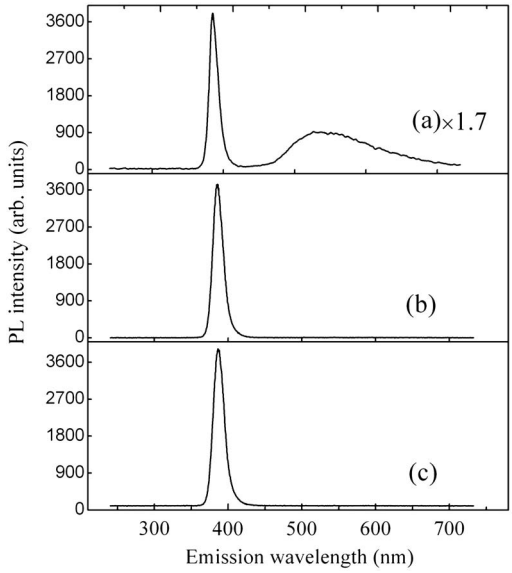

Fig. 2. The room-temperature PL spectra obtained from the ZnO nanowires with and without a-SiN_x:H coating: (a) as-synthesized ZnO nanowires and ZnO nanowires coated with (b)6-nm-thick and (c) 12 nm-thick a-SiN_x:H.

luminescence intensity increased significantly, which indicates that the nonradiative recombination centers in the as-grown ZnO nanowire can be effectively passivated by a-SiN_x:H decoration. Second, the UV emission from the ZnO nanowire coated with a 6-nm-thick a-SiN_x:H layer increases by about 70%, while the green emission is totally eliminated, which is different from that observed in the cases of ZnO coated by polymer or Al_2O_3 in which the green defect emission can only be suppressed to some extent [7–8]. Finally, it is found that the PL peak of the UV band does not show any shift when the thickness of a-SiN_x:H is increased from 0 to 12 nm. We also noted that the increase of the a-SiN_x:H shell-layer thickness from 6 to 12 nm does not enhance the UV emission further. These results imply that the improved UV emission does not result from the quantum confinement of photo-generated carriers inside the ZnO cores but from the suppression of green emission and nonradiative recombination.

To examine the thermal stability, the ZnO-core/a-SiN_x:H-shell nanowires were postannealed in a N_2 atmosphere at different temperatures. Figure 3 presents the PL spectra of the ZnO-core/6-nm-thick a-SiN_x:H-shell nanowires after annealing. After annealing at 400 °C, the intensity of the UV emission shows no reduction as compared to that of the as-grown sample displayed in Fig. 2. Meanwhile, the broad green emission observed in the as-grown sample (uncoated) can be still completely suppressed. It is interesting to find that a negligible green emission can still be seen even though the annealed temperature increases up to 600 °C. These PL behaviors are different from those of the uncoated ZnO nanowire where the intensity of the UV emission is remarkably decreased and the green emission intensity is significantly enhanced after annealing at 400 °C [12]. These results demonstrate that a-SiN_x:H decorating on ZnO nanowire as a protective film effectively improves the thermal stability of ZnO nanowires.

Generally, ZnO material exhibits an n-type characteristic for its intrinsic defects such as oxygen vacancies [6]. The defects after adsorbing the gas molecules would trap free electrons, which results in an upward band bending of the surface and gives rise to a space charge region near

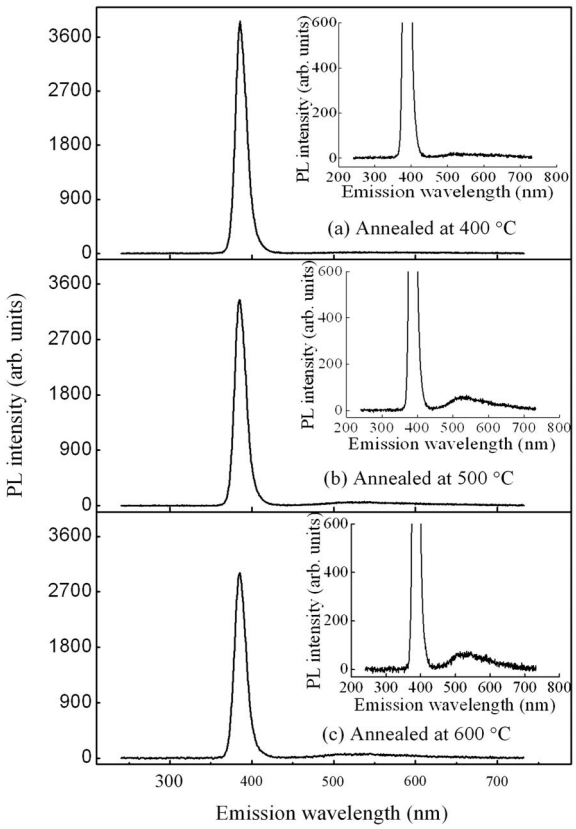

Fig. 3. The PL spectra of the ZnO-core/6-nm-thick a-SiN_x:H-shell nanowires after annealing at 400 °C, 500 °C, and 600 °C for 30 min in an N_2 atmosphere, respectively. Insets show the green emission for the corresponding samples.

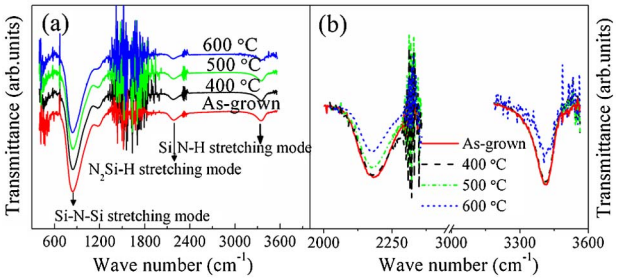

Fig. 4. (Color online) (a) FTIR spectra of the a-SiN_x:H films with and without thermal annealing, respectively. The absorption band at ~850 cm^{-1} is connected with Si–N stretching mode. The ~2140 cm^{-1} band and ~3350 cm^{-1} band are assigned to Si–H and N–H stretching modes, respectively [20]. (b) Absorption bands of Si–H stretching mode and N–H stretching mode.

the ZnO surface. Consequently, it induces the separation of photo-generated electron-hole pairs and leads to a reduction in UV emission intensity [18]. On the other hand, the excess holes at the surface as a result of the upward band bending would tunnel into the deep-level defect centers inside the ZnO nanowires and cause a deep-level defect emission (green emission) [8, 19]. In recent years, Liu *et al.* and Richters *et al.* reported that the UV and deep-level defect emissions could be efficiently controlled by coating PMMA polymer or Al_2O_3 [7–8]. However, it is also found that the deep-level green defect emission in these cases still cannot be totally suppressed at room temperature. In particular, in the case of ZnO treated by plasma, the strong deep-level defect emission would even be recovered after the samples were annealed at temperatures higher than 400 °C [12]. The PL phenomena differ sharply from those observed in our case. As is shown in Fig. 3, the complete suppression of the deep-level defect emission can be obtained from ZnO-core/a-SiN_x:H-shell even annealed at 400 °C. The result strongly suggests that the a-SiN_x:H shell can be used to manipulate optical properties of ZnO nanowires. In our case, the precursors of SiH_4, NH_3, and H_2 were used as source gases to fabricate a-SiN_x:H in the parallel plate radio frequency glow discharge system. In the growth process, the depletion of the precursors through electron impact would produce a large number of H and N radicals flux to the growth surface. This reduces the surface traps and further lowers the surface band bending of ZnO cores. As a result, it leads to a stronger overlap of the wave functions of electrons and holes in the ZnO cores, enhances UV emission, and reduces deep-level defect emission. The H and N radicals located at the defect sites would further react with other radicals such as (Si, H, or N) to form a-SiN_x:H. For the a-SiN_x:H, the Si–H bonds are stable at a annealing temperature of 400 °C while the N–H bonds are still unable to be dissociate even at a high annealing temperature of 500 °C, as is shown in Fig. 4. Therefore, it is very reasonable that PL emission from ZnO-core/a-SiN_x:H-shell nanowire can remain unchanged even when the annealing temperature increases up to 400 °C. Comparing Fig. 3 with Fig. 4, it is clear that the intensity of the UV emission from the ZnO-core/a-SiN_x:H-shell nanowires reduces along with the decrease of the Si–H and N–H vibration intensity, while the intensity of the defect emission exhibits a inverse tendency to that of the Si–H and N–H vibration. Therefore, the small degradation in UV emission as well as the observed weak defect green emission can be ascribed to the H and N desorption from defect states at the ZnO nanowire surface.

In summary, we demonstrated that a-SiN_x:H decoration could tune ZnO nanowire optical properties in a controllable way. The improved PL performances were ascribed to the surface modification by a-SiN_x:H, where H and N atoms play main contributions

Financial support from the Research Grants Council of Hong Kong (projects CityU5/CRF/08, 603408, 604009, and RPC10SC04), National Natural Science Foundation of China (NSFC; 60806046), and technical support of the Rath-HKUST Nanotechnology Laboratory at MCPF (project SEG_HKUST08) are hereby acknowledged.

References

1. M. H. Huang, S. Mao, H. Feick, H. Yan, Y. Wu, H. Kind, E. Weber, R. Russo, and P. Yang, Science **292**, 1897 (2001).
2. Q. Yang, W. Wang, S. Xu, and Z. L. Wang, Nano Lett. **11**, 4012 (2011).
3. S. Chu, G. Wang, W. Zhou, Y. Lin, L. Chernyak, J. Zhao, J. Kong, L. Li, J. Ren, and J. Liu, Nat. Nanotechnol. **6**, 506 (2011).
4. B. D. Yao, Y. F. Chan, and N. Wang, Appl. Phys. Lett. **81**, 757 (2002).
5. H.-Y. Li, S. Ruhle, R. Khedoe, A. F. Koenderink, and D. Vanmaekelbergh, Nano Lett. **9**, 3515 (2009).
6. M. D. McCluskey and S. J. Jokela, J. Appl. Phys. **106**, 071101 (2009).
7. J.-P. Richters, T. Voss, L. Wischmeier, I. Rűckmann, and J. Gutowski, Appl. Phys. Lett. **92**, 011103 (2008).
8. C. Y. Chen, C. A. Lin, M. J. Cen, G. R. Lin, and J. H. He, Nanotechnology **20**, 185605 (2009).
9. K. W. Liu, R. Chen, G. Z. Xing, T. Wu, and H. D. Sun, Appl. Phys. Lett. **96**, 023111 (2010).
10. C. Y. Liu, H. Y. Xu, J. G. Ma, X. H. Li, X. T. Zhang, Y. C. Liu, and R. Mu, Appl. Phys. Lett. **99**, 063115 (2011).
11. L. Shi, Y. Xu, S. Hark, Y. Liu, S. Wang, L. Peng, K. Wong, and Q. Li, Nano Lett. **7**, 3559 (2007).
12. C.-C. Lin, H.-P. Chen, H.-C. Liao, and S.-Y. Chen, Appl. Phys. Lett. **86**, 183103 (2005).
13. X. Meng, H. Peng, Y. Gai, and J. Li, J. Phys. Chem. C **114**, 1467 (2010).
14. A. B. Djurišić, Y. H. Leung, W. C. H. Choy, K. W. Cheah, and W. K. Chan, Appl. Phys. Lett. **84**, 2635 (2004).
15. P. Yang, H. Yan, S. Mao, R. Russo, J. Johnson, R. Saykally, N. Morris, J. Pham, R. He, and H.-J. Choi, Adv. Funct. Mater. **12**, 323 (2002).
16. T.-J. Kuo, C.-N. Lin, C.-L. Kuo, and M. H. Huang, Chem. Mater. **19**, 5143 (2007).
17. J. Tauc, *Amorphous and Liquid Semiconductors* (Springer, 1974).
18. K. Vanheusden, C. H. Seager, W. L. Warren, D. R. Tallant, and J. A. Voigt, Appl. Phys. Lett. **68**, 403 (1996).
19. J.-P. Richters, T. Voss, D. S. Kim, R. Scholz, and M. Zacharias, Nanotechnology **19**, 305202 (2008).
20. F. Giorgis, C. F. Pirri, and E. Tresso, Thin Solid Films **307**, 298 (1997).